Supporting Information

Structure Frustration Enables Thermal History-Dependent Responsive Behavior in Self-Healing Hydrogels

Chengtao Yu[a,b], Kunpeng Cui[c]*, Honglei Guo[d], Ya Nan Ye[e], Xueyu Li[e], and Jian Ping Gong[c,d,e]*

[a]Graduate School of Life Science, Hokkaido University, Sapporo 001-0021, Japan; [b]Institute of Zhejiang University-Quzhou, 78 Jiuhua Boulevard North, Quzhou 324000, China. [c]Institute for Chemical Reaction Design and Discovery (ICReDD), Hokkaido University, Sapporo 001-0021, Japan; [d]Faculty of Advanced Life Science, Hokkaido University, Sapporo 001-0021, Japan; [e]Global Institution for Collaborative Research and Education (GI-CoRE), Hokkaido University, Sapporo 001-0021, Japan.

*Corresponding authors:
Kunpeng Cui, E-mail: kpcui@sci.hokudai.ac.jp
Jian Ping Gong, E-mail: gong@sci.hokudai.ac.jp

Contents

1. Supporting results

1) Chemical structure of the monomers and of the hydrogels

A recent work[1] studied the reactivity ratios of NaSS ($r_1 = 1.26$) and DMAEA-Q ($r_2 = 0.58$) in water and analyzed the instantaneous number-average sequence length of the NaSS monomer, N_{NaSS}, and DMAEA-Q monomer, $N_{DMAEA\text{-}Q}$, with the total monomer conversion p according to the Mayo–Lewis theory. At total monomer conversion $p = 0$, the determination of N_{NaSS} is 2.4 and $N_{DMAEA\text{-}Q}$ is 1.5. This can be understood that, as an average of the incorporation to the growing polymer chains, a sequence of three NaSS molecules follows by two DMAEA-Q molecules. At $p = 0.7$, then $N_{NaSS} = 1.4$ and $N_{DMAEA\text{-}Q} = 2.7$, a sequence of one NaSS molecule would follow by three DMAEA-Q molecules. At higher convention ($p > 0.9$), the polymer chains will grow with a block sequence of DMAEA-Q molecules. So, NaSS rich segments formed at the beginning of polymerization and DMAEA-Q-rich segments formed at the end of polymerization.

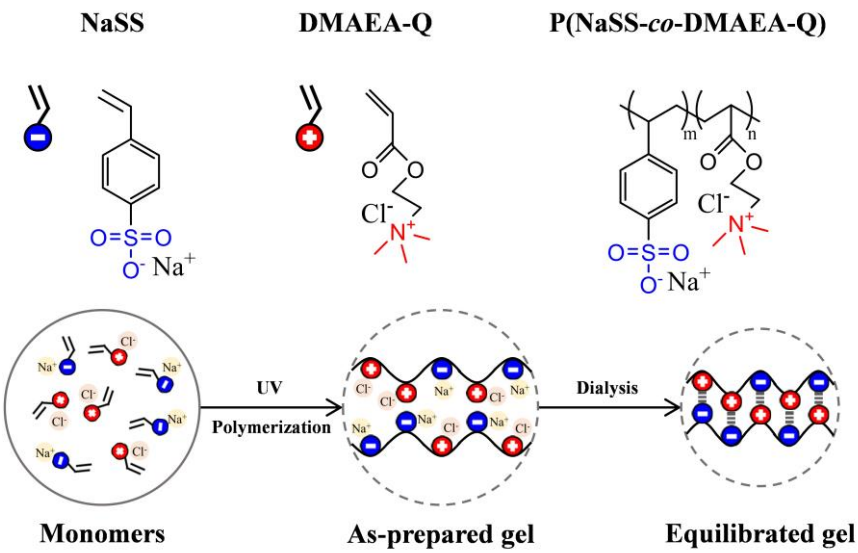

Fig. S1. Schematic illustration of the chemical structure of the monomers NaSS and DMAEA-Q, and the P(NaSS-*co*-DMAEA-Q) hydrogel.

2) Structure analysis

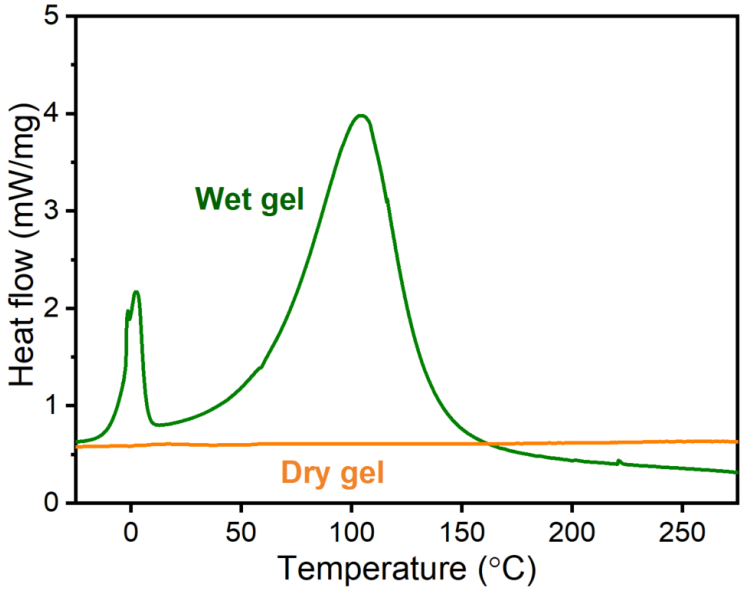

Fig. S2. Differential scanning calorimetry (DSC) scanning for dry and wet P(NaSS-co-DMAEA-Q) samples performed at a heating rate of 10 °C/min from -50 °C to 275 °C. The two peaks (around 0 °C and 100 °C) in the DSC curve of wet sample are assigned to the melting point and boiling point of water in the polymer, respectively. No thermal melting peak from the ion complex structures appears in DSC curves either for the hydrogels or for the dried sample. This result indicates that the PA gel is amorphous with no crystalline structure.

3) Transmittance change of the PA gel during heating and recovery

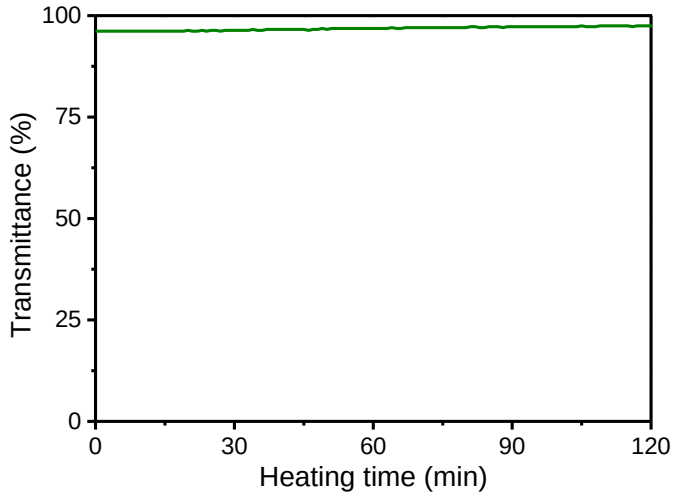

Fig. S3. Transmittance of the gel during heating at T_L = 80 °C for t_L = 2 h.

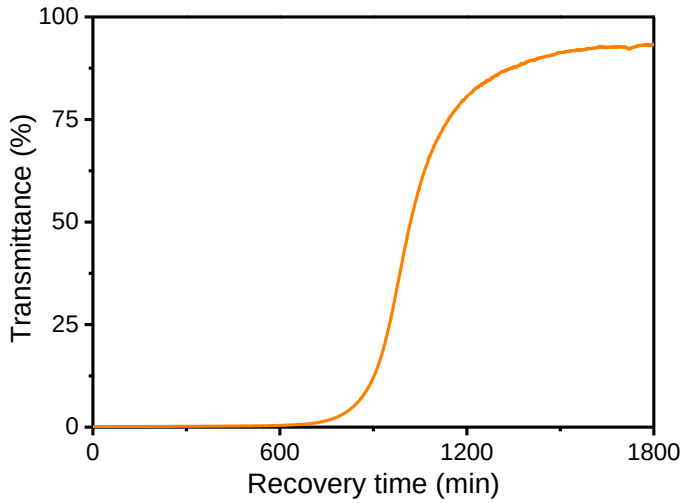

Fig. S4. Transmittance of the gel during recovery at T_F = 25 °C. The turbid gel was obtained by quenching the gel to 25 °C after heating at T_L = 80 °C for t_L = 2 h.

4) Small size change during thermal response

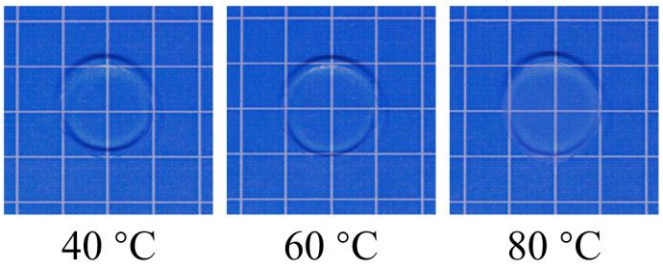

Fig. S5. Optical images of a PA gel at different heating temperatures for T_L = 2 h. Background lattices, 5 mm.

5) Effect of heating temperature and cooling temperatures on transmittance of PA gels at cooling

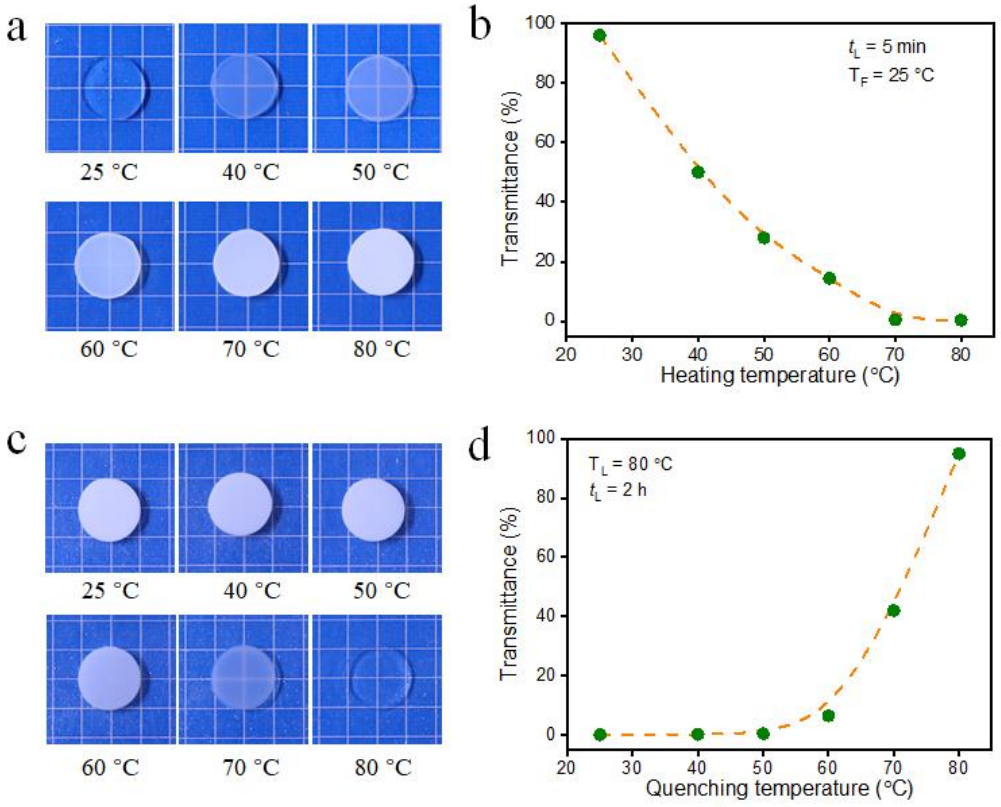

Fig. S6. Tunable transparency of PA gels at cooling by tuning T_L and T_F. (a) Optical images and (b) transmittance change of PA gels with different heating temperatures T_L for fixed t_L = 5 min and T_F = 25 °C. (c) Optical images and (d) transmittance change of PA gels with different T_F for fixed T_L = 80 °C and t_L = 5 min. The optical images were taken after cooling the temperature to T_F for 1 min. The temperatures in (a) and (c) are T_L and T_F, respectively. Background lattices, 5 mm.

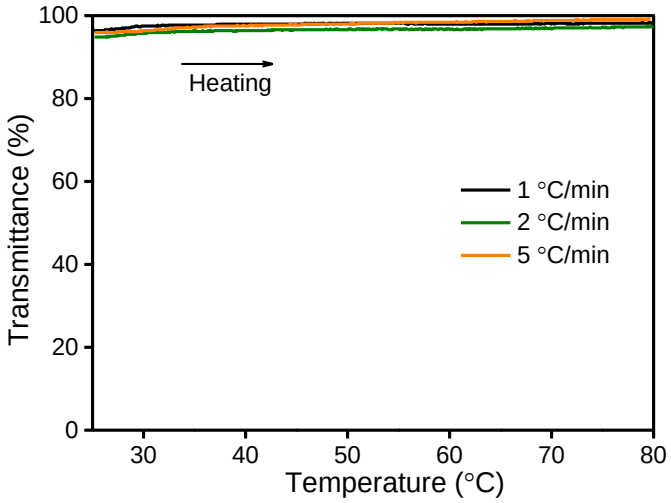

Fig. S7. Transmittance of the original gel during heating from 25 to 80 °C with different heating rates.

6) Comparison of mechanical performances of turbid and original gels

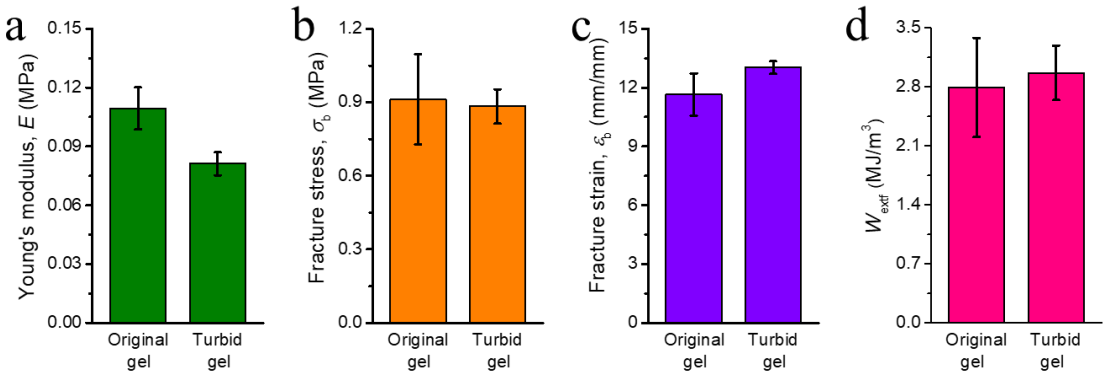

Fig. S8. Tensile behavior of original gel and turbid gel. (a) Young's modulus E, (b) fracture stress σ_b, (c) fracture strain ε_b, and (d) work of extension at fracture W_{extf}, calculated from the tensile stress-strain curves.

Fig. S8 exhibits the Young's modulus E, fracture stress σ_b, fracture strain ε_b, and work of extension at fracture W_{extf}, calculated from the uniaxial tensile stress-strain curves of the original gel and the turbid gel at 25 °C (Fig. 6b, main text). As the total water contents (W_T's) of the turbid gel (55.0%±0.8%) and the original gel (45.7%±0.3%) are different[2], we calculated their polymer volume fractions (ϕ_p) to remove this effect. ϕ_p of the gels is calculated by the equation

$$\phi_p^{-1}=1+[W_T/(1-W_T)]/(\rho_p/\rho_W),$$

where ρ_p = 1.19 and ρ_W = 0.98 g/cm^3 are the densities of PA and water at room temperature, respectively.[3] ϕ_p of the original gel and turbid gel are 0.50 and 0.41, respectively (Fig. S9). By assuming the polymer density changes of the original gel and the turbid gel are homogeneous, E, σ_b, and ε_b are related to ϕ_p: $E=E^N\phi_p$, $\sigma_b=\sigma_b^N\phi_p^{2/3}$, and $\lambda_b=\lambda_b^N\phi_p^{1/3}$, where E^N, σ_b^N, and λ_b^N are the values at the virtual

reference state (ϕ_p = 1).[4] Here, $\lambda_b = \varepsilon_b + 1$ is the fracture stretch ratio. E^N, σ_b^N, and ε_b^N of the original gel and the turbid gel are almost the same (Figs. 6c-e, main text).

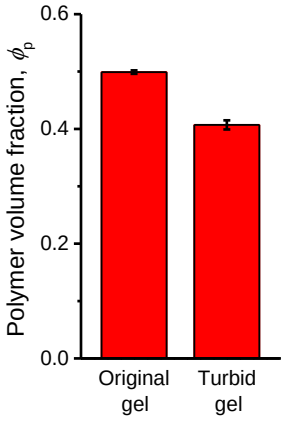

Fig. S9. Polymer volume fractions of original gel and turbid gel.

Single-edge notch test was performed to evaluate the toughness of the original gel and the turbid gel.[5] The toughness represented by fracture energy Γ is estimated and shown in Fig. S10. Similarly, fracture energy Γ of the turbid and original gels at the virtual reference state (ϕ_p = 1) is obtained by $\Gamma=\Gamma^N\phi_p^{2/3}$. Γ^N are about 2.5±0.2 kJ/m^2 for the turbid gel and 3.0±0.2 kJ/m^2 for the original gel (Fig. 6g, main text), respectively, which are nearly the same. Therefore, all the mechanical tests in this work suggest that the mechanical performance of PA gels can keep almost unchanged before and after thermal treatment.

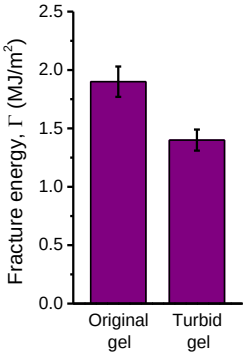

Fig. S10. Fracture energy Γ of original gel and turbid gel.

7) Comparison of uniaxial tensile behavior of the original gels with and without a flaw

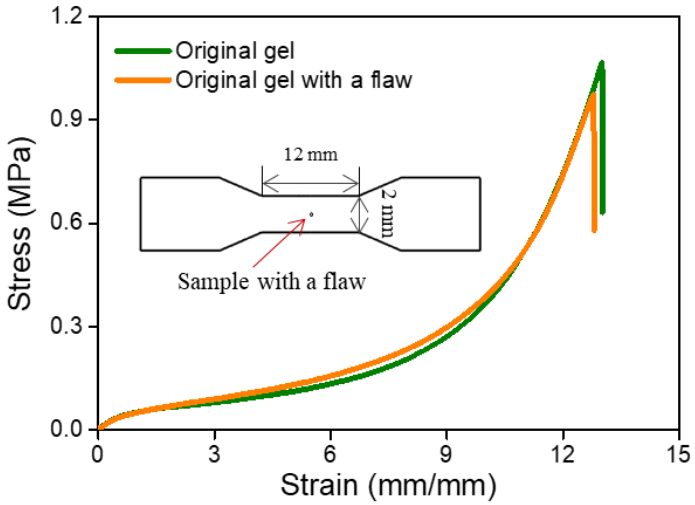

Fig. S11. Comparison of the uniaxial tensile behavior of the original gels with and without a flaw. Inset shows a dumbbell shape sample with a 0.25 mm diameter flaw in the center of the sample. The gels with and without a flaw show nearly the same tensile behavior, indicates that the PA gel is flaw insensitive up to a size of submillimeter. This explains why the turbid gel containing water aggregations with a size of several micrometers has similar mechanical performance to the original gel.

2. Supporting movie

Movie S1. Movie to show the autonomic disappearance of the recorded temporary information on the surface of PA gels. A letter “L” is initially written on the surface of the gel; after 30 s, “S” is written, and L nearly disappears at this time; then, “W” is written after waiting another 30 s, and S almost disappears; finally, W also disappears, and the PA gel turns to transparent as before.

3. Supporting references

(1) Wu, S.; Shao, Z.; Xie, H.; Xiang, T.; Zhou, S. Salt-Mediated Triple Shape-Memory Ionic Conductive Polyampholyte Hydrogel for Wearable Flexible Electronics. *J. Mater. Chem. A* **2021**, *9* (2), 1048–1061.

(2) Yu, C.; Guo, H.; Cui, K.; Li, X.; Ye, Y. N.; Kurokawa, T.; Gong, J. P. Hydrogels as Dynamic Memory with Forgetting Ability. *Proc. Natl. Acad. Sci. U. S. A.* **2020**, *117* (32), 18962–18968.

(3) Sun, T. L.; Luo, F.; Kurokawa, T.; Karobi, S. N.; Nakajima, T.; Gong, J. P. Molecular Structure of Self-Healing Polyampholyte Hydrogels Analyzed from Tensile Behaviors. *Soft Matter* **2015**, *11* (48), 9355–9366.

(4) Itagaki, H.; Kurokawa, T.; Furukawa, H.; Nakajima, T.; Katsumoto, Y.; Gong, J. P. Water-Induced Brittle-Ductile Transition of Double Network Hydrogels. *Macromolecules* **2010**, *43* (22), 9495–9500.

(5) Long, R.; Hui, C. Y. Fracture Toughness of Hydrogels: Measurement and Interpretation. *Soft Matter* **2016**, *12* (39), 8069–8086.